Heliyon 10 (2024) e29401

Contents lists available at ScienceDirect

Heliyon

journal homepage: www.cell.com/heliyon

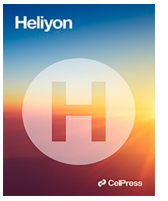

Research article

Uncovering a novel DNA repair-related radiosensitivity model for evaluation of radiotherapy susceptibility in uterine corpus endometrial cancer

Hainan Yang [a], Yanru Qiu [b], Junjun Chen [c], Jinzhi Lai [b,*]

[a] Department of Ultrasound, First Affiliated Hospital of Xiamen University, Xiamen, Fujian, 361003, China
[b] Department of Oncology, The Second Affiliated Hospital of Fujian Medical University, Quanzhou, Fujian, 362000, China
[c] National Health Commission (NHC) Key Laboratory of Personalized Diagnosis and Treatment of Nasopharyngeal Carcinoma, Jiangxi Cancer Hospital of Nanchang Medical College, Nanchang, Jiangxi, 330000, China

ARTICLE INFO

Keywords:
Uterine corpus endometrial cancer
Radiotherapy
Radiosensitivity
DNA repair-related genes
PD-L1

ABSTRACT

Background: Uterine corpus endometrial cancer (UCEC) exhibit heterogeneity in their DNA repair capacity, which can impact their response to radiotherapy. Our study aimed to identify potential DNA repair-related biomarkers for predicting radiation response in UCEC.
Methods: We conducted a thorough analysis of 497 UCEC samples obtained from TCGA database. Using LASSO-COX regression analysis, we constructed a radiosensitivity signature and subsequently divided patients into the radiosensitive (RS) and the radioresistant (RR) groups based on their radiosensitivity index. The GSVA and GSEA were performed to explore functional annotations. The CIBERSORT and ESTIMATE algorithms were utilized to investigate the immune infiltration status of the two groups. Additionally, we utilized the Tumor Immune Dysfunction and Exclusion (TIDE), Immunophenotype Score (IPS), and pRRophetic algorithms to predict the effectiveness of different treatment modalities.
Results: We constructed a radiosensitivity index consists of four DNA repair-related genes. Patients in the RS group demonstrated significantly improved prognosis compared to patients in the RR group when treated with radiotherapy. We observed that the RS group exhibited a higher proportion of the POLE ultra-mutated subtype, while the RR group had a higher proportion of the copy number high subtype. GSVA enrichment analysis revealed that the RS group exhibited enrichment in DNA damage repair pathways. Notably, the RS group demonstrated a higher proportion of naïve B cells and follicular helper T cells, while regulatory T cells (Tregs) and memory B cells were more abundant in the RR group. Furthermore, patients in the RS-PD-L1-high subgroup exhibited enrichment in immune-related pathways and increased sensitivity to immunotherapy, which is likely to contribute to their improved prognosis. Additionally, we conducted in vitro experiments to validate the expression of radiosensitivity genes in non-radioresistant (AN3CA) and radioresistant (AN3CA/IR) endometrial cancer cells.
Conclusions: In conclusion, our research successfully constructed a radiosensitivity signature with robust predictive capacity. These findings shed light on the association between immune activation, PD-L1 expression, and the response to immunotherapy in the context of radiotherapy.

* Corresponding author.
E-mail address: laijinzhi2017@fjmu.edu.cn (J. Lai).

https://doi.org/10.1016/j.heliyon.2024.e29401
Received 18 September 2023; Received in revised form 16 December 2023; Accepted 8 April 2024
Available online 9 April 2024

1. Introduction

Uterine corpus endometrial cancer (UCEC) is a type of malignant tumor that originates from the epithelial cells of the endometrium [1]. It is the most common malignancy of the female reproductive system in developed countries and some urban areas [2]. Over the past few decades, the incidence of endometrial cancer has shown a consistent increase or stabilization, especially in South Africa and some Asian countries. According to data from the National Cancer Center of China, the incidence rate of UCEC experienced a significant annual increase of 2.6 %, while the mortality rate exhibited a noteworthy annual decrease of 1.9 % between 2007 and 2016. In 2016, there were approximately 71,100 newly diagnosed cases of UCEC in China, accounting for 3.8 % of all female cancer cases and 27.5 % of gynecological malignancies. The number of deaths was 17,100, accounting for 1.9 % of all female cancer deaths and 20.4 % of gynecological malignancy deaths [3]. These presented statistics underscore the significant health impact and substantial public health challenge posed by UCEC.

Radiotherapy is a fundamental treatment modality for UCEC, playing a crucial role in reducing the risk of local recurrences following surgery [4]. Although radiotherapy has proven effective in preventing tumor recurrences, there remains a possibility of treatment failure, leading to patterns of both local and distant recurrences [5]. Understanding the molecular mechanisms that contribute to radiosensitivity in UCEC is still an area of ongoing investigation. As such, our study aimed to elucidate the molecular determinants underlying the development of resistance and identify potential biomarkers for predicting radiation response in UCEC. Currently, there is a growing consensus regarding the positive association between DNA damage repair pathways and radiosensitivity in UCEC [6]. Therefore, investigating the expression patterns associated with radio-resistance has the potential to serve as predictive biomarkers for assessing the response to radiotherapy in UCEC patients.

DNA damage is a crucial factor that significantly influences the response to radiation. The effectiveness of radiotherapy primarily relies on its ability to induce cell death through the induction of DNA damage [7]. Consequently, tumor cells equipped with highly efficient DNA damage response mechanisms tend to exhibit radio-resistance, while cancer cells with impaired DNA repair pathways are more likely to be radiosensitive [8]. The characterization of DNA repair-related genes has shed light on their connection with the radiosensitivity of UCEC. Recently, there has been a growing emphasis on identifying radiosensitivity biomarkers at the genomic level, with the aim of enhancing the efficacy of radiotherapy [9]. Therefore, it may be possible to identify DNA repair-related signature that can reliably predict the response to radiotherapy. However, to date, no study has thoroughly investigated the potential of DNA repair-related signatures as predictors for UCEC.

In our study, we conducted an analysis of DNA repair-related genes in UCEC patients, utilizing data obtained from The Cancer Genome Atlas (TCGA) database, a comprehensive resource that profiles the molecular characteristics of various types of cancer. Through this analysis, we constructed a radiosensitivity signature that could effectively predict the response to radiotherapy. The performance of this signature was evaluated by stratifying UCEC patients based on their radiosensitivity index. Notably, the patients classified as radiosensitive (RS) exhibited a significantly improved prognosis compared to those categorized as radioresistant (RR) when subjected to radiotherapy. Moreover, our findings demonstrated that both the radiosensitivity signature and PD-L1 expression status held promise as predictive factors for the response to radiotherapy. These results contribute to our understanding of the optimal combination of treatment modalities with radiotherapy in order to enhance therapeutic outcomes.

2. Materials and methods

2.1. UCEC data sets and preprocessing

We obtained gene-expression data (FPKM normalized) from TCGA through the UCSC Xena browser (https://gdc.xenahubs.net). The data analysis was conducted using R (version 4.1.3) and R Bioconductor packages. To ensure the reliability of the clinical information, samples without complete clinical information, those with survival times less than 30 days, and samples from metastatic tumors were excluded from the analysis. As a result, a total of 497 patients were included in the study population. The stemness scores (mRNAsi) of the UCEC samples were acquired from a previous study [10]. Somatic mutation data in mutation annotation format (MAF) for the 497 UCEC patients were downloaded from the TCGA database. Furthermore, we acquired copy number alteration (CNV) data for the UCEC patients from the TCGA database. To effectively visualize these alterations at the chromosomal level, we employed Circos plots using the RCircos R package [11].

2.2. Development of the DNA repair-related radiosensitivity signature

Firstly, we conducted univariate Cox regression analysis to identify specific DNA repair-related genes (DRGs) that showed a significant association with overall survival (OS) in the radiotherapy group, but not in the non-radiotherapy group or the entire cohort. After that, only patients in the radiotherapy group were selected for the construction of a radiosensitivity signature. To construct the radiosensitivity signature, we utilized LASSO and stepwise Cox regression analysis based on DRGs. The radiosensitivity index of UCEC patients was calculated using the following formula: radiosensitivity index = (Expression gene 1 $\times$ Coefficient gene 1) + (Expression gene 2 $\times$ Coefficient gene 2) + $\cdots$ + (Expression gene n $\times$ Coefficient gene n). We divided the patients into the high-index group and the low-index group according to the median value of the radiosensitivity index. The low-index group, referred to as the RS group, exhibited improved survival after receiving radiotherapy compared to those who did not receive radiotherapy. Conversely, the high-index group, representing patients with a higher radiosensitivity index, was designated as the RR group.

2.3. Functional enrichment analyses

To evaluate the relative enrichment of gene sets between the RS and RR groups, we employed the GSVA method via the GSVA R package [12]. In order to perform this analysis, we obtained the KEGG canonical pathways gene set ('c2.cp.kegg.v2023.1.Hs.symbols') from the Molecular Signatures Database (MSigDB) and selected it as the background gene set. This gene set represents the Kyoto Encyclopedia of Genes and Genomes (KEGG) pathways based on curated gene-pathway associations [13]. Additionally, we utilized Gene Set Enrichment Analysis (GSEA) to identify the biological processes (BP), molecular functions (MF), and cellular components (CC) that were significantly enriched in either the RS or RR group. We applied an adjusted p-value threshold of less than 0.05 to determine the statistical significance of the enrichment analysis.

2.4. Immune infiltration analyses

In this study, we employed the CIBERSORT algorithm, available in the "CIBERSORT" R package, to estimate the relative abundances of 22 distinct immune cell types in each sample [14]. To identify significant results for further analysis, we considered a p-value threshold of $\leq$0.05 for further analysis [14,15]. We analyzed the expression patterns of 29 immunity-related signatures, representing various immune cell functions and pathways, utilizing the single-sample Gene Set Enrichment Analysis (ssGSEA) algorithm available in the "GSEAbase" and "GSVA" R packages [16]. Furthermore, we employed the "ESTIMATE" algorithm, implemented in the "estimate" R package, to estimate the immune score, stromal score, and tumor purity for each sample [17]. The TIMER [18], QUANTISEQ [19], EPIC [20] and XCELL [21] algorithms were applied to calculate the abundances of immune cells between the RS and RR groups.

2.5. Drug sensitivity analyses

The immunophenotype scores (IPS) were used as a predictive measure to predict a patient's response to immune checkpoint inhibitor-based immunotherapy [22]. IPS values for UCEC patients were obtained from The Cancer Immunome Atlas (TCIA) database (https://tcia.at/home), which uses machine learning techniques to develop a scoring scheme for quantification. We used the Tumor Immune Dysfunction and Exclusion (TIDE) algorithm (http://tide.dfci.harvard.edu/) to assess patients' responsiveness to immunotherapy. The TIDE algorithm evaluates T-cell dysfunction and exclusion scores, derived from gene expression profiles, to predict the likelihood of patients' response to immune checkpoint inhibitor therapy [23]. The pRRophetic algorithm predicts the efficacy of patients' response to chemotherapeutic and targeted therapy by evaluating the half maximal inhibitory concentration (IC50) for each UCEC patient. IC50 values were obtained from the Genomics of Drug Sensitivity in Cancer (GDSC) database [24].

2.6. Establishment and assessment of radioresistant AN3CA/IR cell line

The human endometrial cancer cell line AN3CA was purchase from the China Center for Type Culture Collection (CCTCC, Wuhan, China). The AN3CA cells was cultured in DMEM medium (Corning, United States) supplemented with 10 % fetal bovine serum (Corning, United States) and 1 % antibiotics (Gibco-BRL, Gaithersburg, MD, United States). The cells were incubated at 37 °C with saturated humidity and 5 % CO2. Prior to experimentation, AN3CA cells were screened for mycoplasma contamination. To establish radioresistant AN3CA/IR cells, AN3CA cells were repeatedly exposed to radiation. Briefly, AN3CA cells were intermittently irradiated with a single dose of 2, 4, 6, 8, 10, 10, and 10 Gy, totaling a cumulative irradiation dose of 50 Gy [25]. The radio-resistance of AN3CA/IR was assessed through cell proliferation assays. The radio-resistance of AN3CA/IR cells was evaluated through the Cell Counting Kit-8 (CCK-8) assay. AN3CA/IR cells were seeded in 96-well plates and incubated. After 24 h, the cells were exposed to either 4 or 8 Gy of irradiation. Then, 10 μl of CCK-8 solution (Dojindo, Kumamoto, Japan) was added to the cells, followed by a 3-h incubation. The optical density at 450 nm was measured using a microplate reader.

2.7. Quantitative real-time polymerase chain reaction (qRT-PCR)

The RNA extraction procedure employed Trizol reagent in accordance with the manufacturer's protocol (Invitrogen, San Diego, CA, USA). The concentration of the extracted RNA was quantified using a NanoDrop 2000 spectrophotometer (ThermoFisher, USA). Subsequently, cDNA synthesis was executed utilizing the Transcriptor First Strand cDNA Synthesis Kit (Roche, Germany) with the RNA samples. For quantitative real-time PCR (RT-qPCR), the SYBR Prime Script RT−PCR Kit (Invitrogen, USA) was utilized, and the primer sequences can be found in Table S1. All experiments were carried out in triplicate, and the Ct values were normalized using the genomic mean of the internal control, GAPDH. The relative expression levels were calculated using the $2^{-\Delta\Delta CT}$ method, and the results were presented as fold change relative to the internal control genes. To ensure accuracy and reliability, the data presented in this study were derived from three independent experiments.

2.8. Statistical analysis

The analysis of data in this study was conducted using R software version 4.1.3. The Chi-square test was utilized to compare categorical and pairwise features among different groups. For comparing normally distributed data between two groups, the student's t-test was employed. The Mann-Whitney *U* test was applied to determine statistically significant differences between two groups. In cases where there were multiple independent groups, the Kruskal-Wallis test was applied. Pearson's correlation test was employed to

investigate associations between variables that demonstrated a normal distribution. Conversely, Spearman's correlation test was utilized to assess relationships between variables that deviated from a normal distribution. To analyze disparities in survival outcomes among two or more groups, the Kaplan-Meier method and log-rank test were applied. All statistical tests conducted in this study were two-tailed, ensuring the examination of both positive and negative associations. A p-value below the threshold of 0.05 was considered statistically significant, indicating that the observed results were unlikely to occur by chance. This significance level was utilized unless otherwise specified or stated in the analysis.

3. Results

3.1. Developing a radiosensitivity signature using DNA repair-related genes

The study's workflow was depicted in Fig. S1. Firstly, we performed a univariate Cox regression analysis to detect prognostic DNA

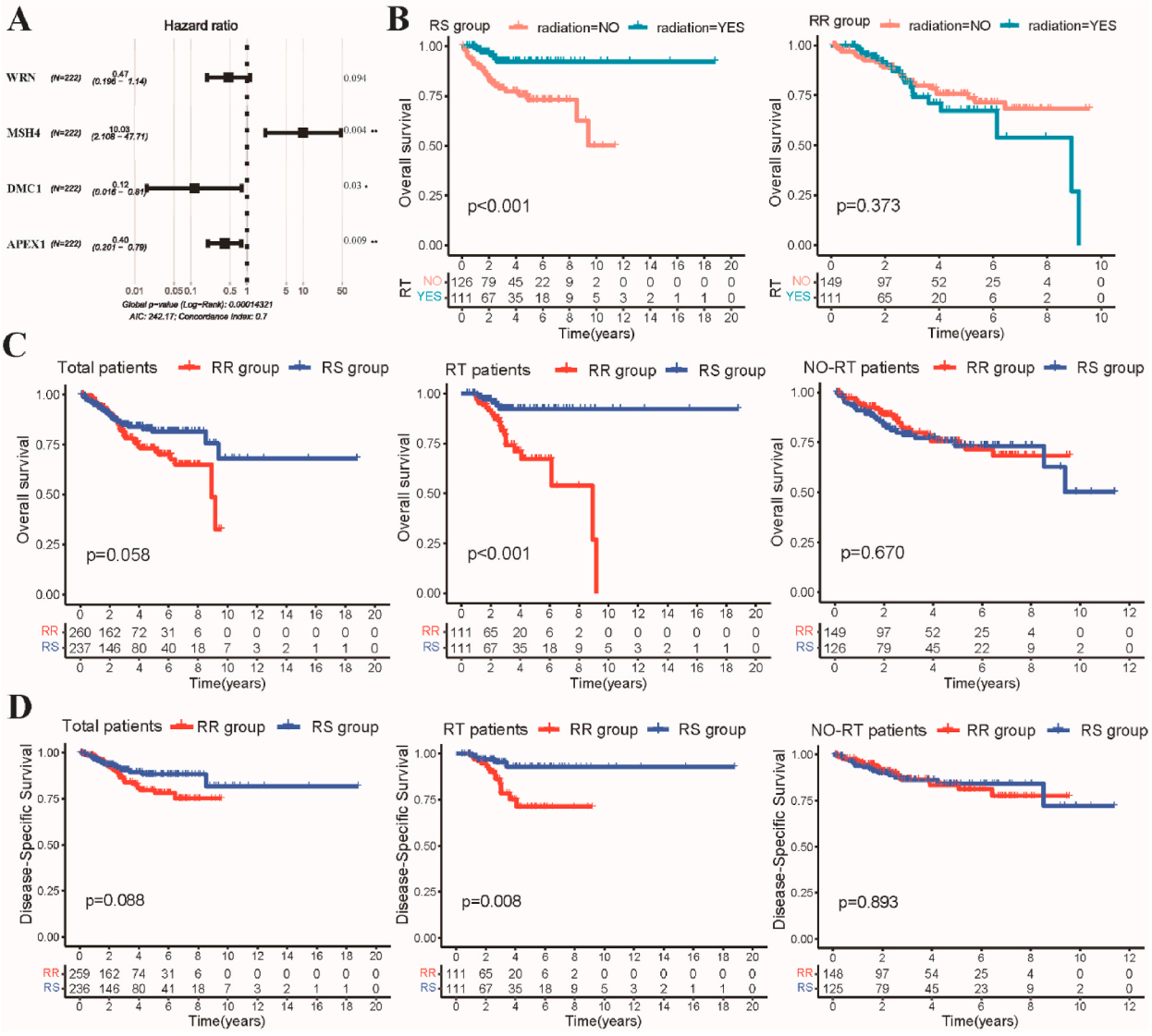

Fig. 1. Development of the DRGs radiosensitivity signature in the TCGA-UCEC dataset. **(A)** Forest plot displaying the results of the multivariate Cox regression analysis conducted in the cohort of radiotherapy patients. **(B)** The Kaplan-Meier plot demonstrates the OS outcomes of patients categorized into RS groups, comparing those who received radiotherapy to those who did not. Notably, there were no significant differences in OS rates observed between radiotherapy and non-radiotherapy patients within the RR group. **(C)** Kaplan-Meier survival curves illustrate the OS outcomes of patients in both the RS and RR groups, within the subsets of patients who underwent radiotherapy, those who did not undergo radiotherapy, and the total patient cohort. **(D)** Kaplan-Meier survival curves depict the DSS outcomes of patients in both the RS and RR groups, within the subsets of patients who received radiotherapy, those who did not receive radiotherapy, and the total patient cohort. *p < 0.05, **p < 0.01.

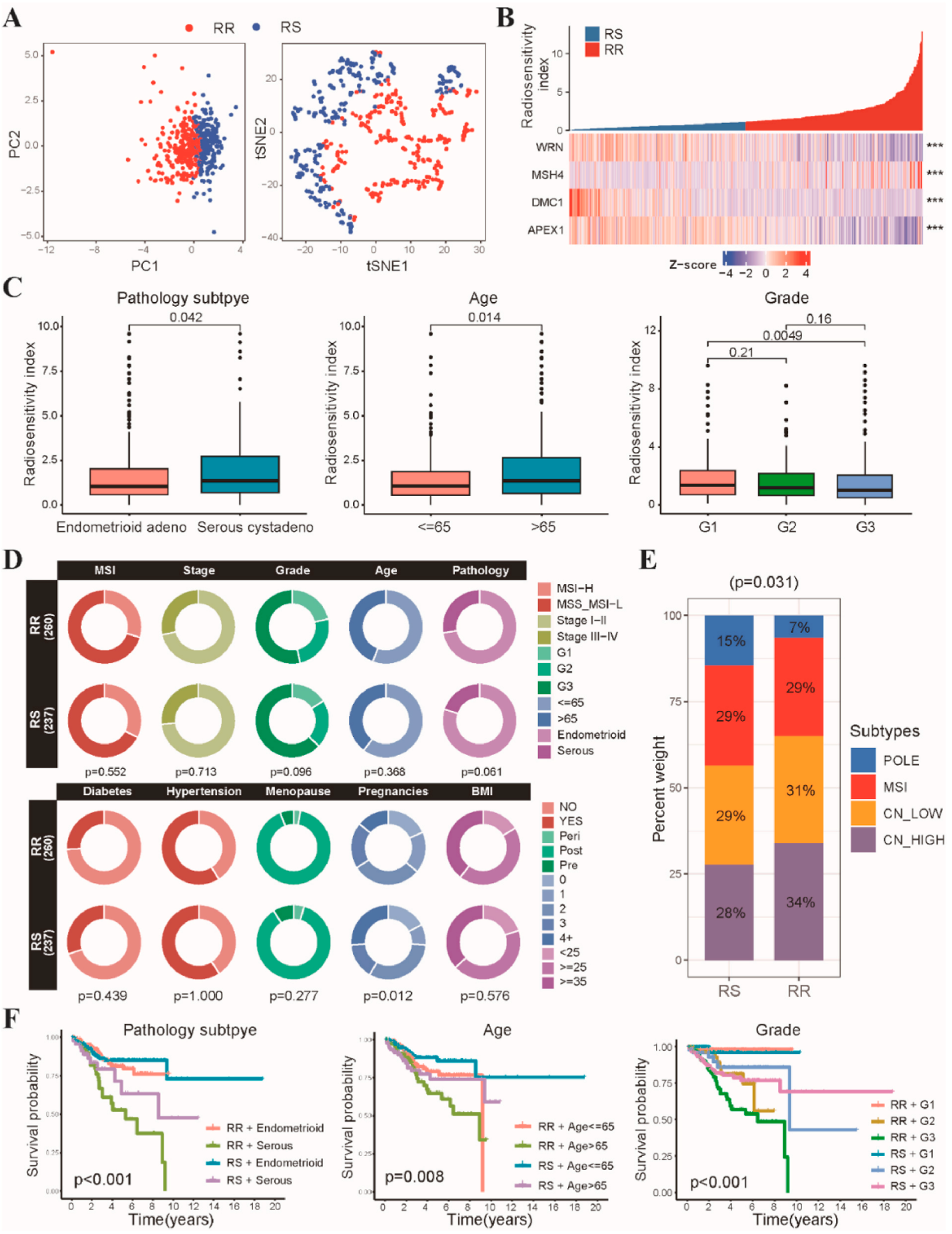

(caption on next page)

Fig. 2. Correlation between radiosensitivity signature and pathological factors in the TCGA-UCEC dataset. (A) The PCA and tSNE plots visually illustrate the distribution patterns of patients in the RS and RR groups based on the radiosensitivity gene signature of four genes in TCGA-UCEC patients. **(B)** The heatmap highlights significant differences in gene expression levels of the four-gene radiosensitivity index between the two groups. **(C)** The boxplot demonstrated that patients with endometrioid adenocarcinoma, low grade, and aged <65 years exhibit lower radiosensitivity index values compared to patients with serous cystadenocarcinoma, high grade, and aged ≥65 years. **(D)** The circus plot provides a visual representation of the correlation between radiosensitivity index and various clinical characteristics. **(E)** Stacked histogram displaying the proportions of molecular subtypes in RS and RR groups. **(F)** Kaplan-Meier survival analysis reveals a significantly poorer prognosis for patients in the RR group with serous cystadenocarcinoma, G3 grade, and aged ≥65 years. ***p < 0.001.

repair-related genes in both radiotherapy (RT) and non-radiotherapy (Non-RT) patients using the TCGA-UCEC dataset. Our analysis revealed that 13 DRGs were significantly associated solely with OS in radiotherapy patients, while no significant association was found in non-radiotherapy patients or in the total cohort (Figs. S2A–B). Next, we utilized LASSO Cox regression analysis specifically for radiotherapy patients to develop a radiosensitivity signature (Fig. S2C). This analysis identified 4 key genes that were essential for constructing the radiosensitivity signature (Fig. 1A). By applying the median radiosensitivity index (RSI) derived from this signature in radiotherapy patients, we categorized the total TCGA-UCEC cohort into low-risk and high-risk groups. The formulation of this signature can be found in. Table S2 We further investigated the Kaplan-Meier survival curve to examine the impact of radiotherapy on OS in relation to the radiosensitivity signature. The results showed that patients in the low-risk group who received radiotherapy had significantly improved OS compared to non-radiotherapy patients, whereas no significant difference was observed between radiotherapy and non-radiotherapy patients in the high-risk group (Fig. 1B). Thus, the low-risk group was designated as the RS group, and the high-risk group as the RR group. Moreover, our findings revealed that among radiotherapy patients in the RS group demonstrated significantly improved OS compared to those in the RR group or the total UCEC patient cohort (Fig. 1C). In addition, our analysis of disease-specific survival (DSS) demonstrated that radiotherapy patients in the RS group had better outcomes compared to those in the RR group (Fig. 1D). Overall, our findings collectively demonstrate the potential utility of the radiosensitivity index as a valuable signature for predicting the response to radiotherapy in patients with UCEC.

3.2. Correlation between radiosensitivity signature and clinicopathological factors

The clinicopathological characteristics of patients in the two groups were presented in Table S3. To assess the differences between groups, PCA and tSNE were performed using the expression levels of the radiosensitivity signature. The results revealed a significant divergence in the distribution patterns between the RS and RR groups (Fig. 2A). Furthermore, differential expression analysis demonstrated significant variations in the expression levels of the four identified DRGs between the RS and RR groups (Fig. 2B). Further analysis was conducted to investigate the correlation between the radiosensitivity index and clinicopathological characteristics. Notably, patients with endometrioid adenocarcinoma, low grade, and aged <65 years exhibited a lower radiosensitivity index compared to patients with serous cystadenocarcinoma, high grade, and aged ≥65 years (Fig. 2C). While there were no significant differences in most clinical characteristics between the RS and RR groups, except in the number of pregnancies (Fig. 2D). The RS group primarily consisted of patients who had experienced at least four pregnancies (Fig. S2D). Furthermore, we found that RS group exhibited higher proportions of POLE ultra-mutated subtype, while RR group exhibited higher proportions of copy number high subtype (Fig. 2E). Notably, Kaplan-Meier survival analysis revealed a poorer prognosis for patients in the RR group with serous cystadenocarcinoma, G3 grade, and aged ≥65 years (Fig. 2F). In summary, our results suggest that the radiosensitivity index appears to be negatively correlated with tumor grade and age. Pathological subtypes such as endometrioid adenocarcinoma and the POLE ultra-mutated subtype appear to be sensitive to radiotherapy.

3.3. Landscape of tumor mutational profile between RS and RR groups

We proceeded to analyze the gene mutation data of UCEC patients. The TMB level did not show any significant differences between the RS and RR groups (Fig. S3A). A comprehensive analysis of the gene mutation data revealed that missense mutations were the most frequent, with SNPs being the most common type of mutation (Fig. 3A). The landscape of the mutational profile, focusing on the top 10 mutated genes, is presented in (Fig. 3B). In UCEC patients, PTEN, PIK3CA, and ARID1A were found to be the most frequently mutated genes. The correlation diagram highlighted a dominant co-occurrence relationship among these mutant genes (Fig. 3C). Additionally, there was a higher frequency of mutations in mismatch repair genes, including MLH1, MSH2, MSH6, and PMS2, in the RS group compared to the RR group. Notably, the mutation of MSH6 was significantly enriched in the RS group (Fig. 3D). We also compared the stemness index (mRNAsi) between the RS group and RR group and found that the mRNAsi value was significantly higher in the RS group (Fig. 3E). Furthermore, we provided an illustration depicting the specific chromosomal locations where CNVs impacted the four DNA repair-related genes. The analysis revealed that APEX1 and DMC1 exhibited copy number amplification, while MSH4 and WRN displayed significant CNV deletions, suggesting an increase or loss in the number of copies of these genes (Fig. 3F).

3.4. Functional enrichment analysis of radiosensitivity signature

In order to gain deeper insights into the molecular mechanisms underlying the radiosensitivity signature in UCEC, we conducted GSVA enrichment to assess the differences in pathway activities between RS group and RR group. The enrichment analysis showed that the RS group exhibited significant enrichment in DNA damage repair pathways, including homologous recombination (HR), non-

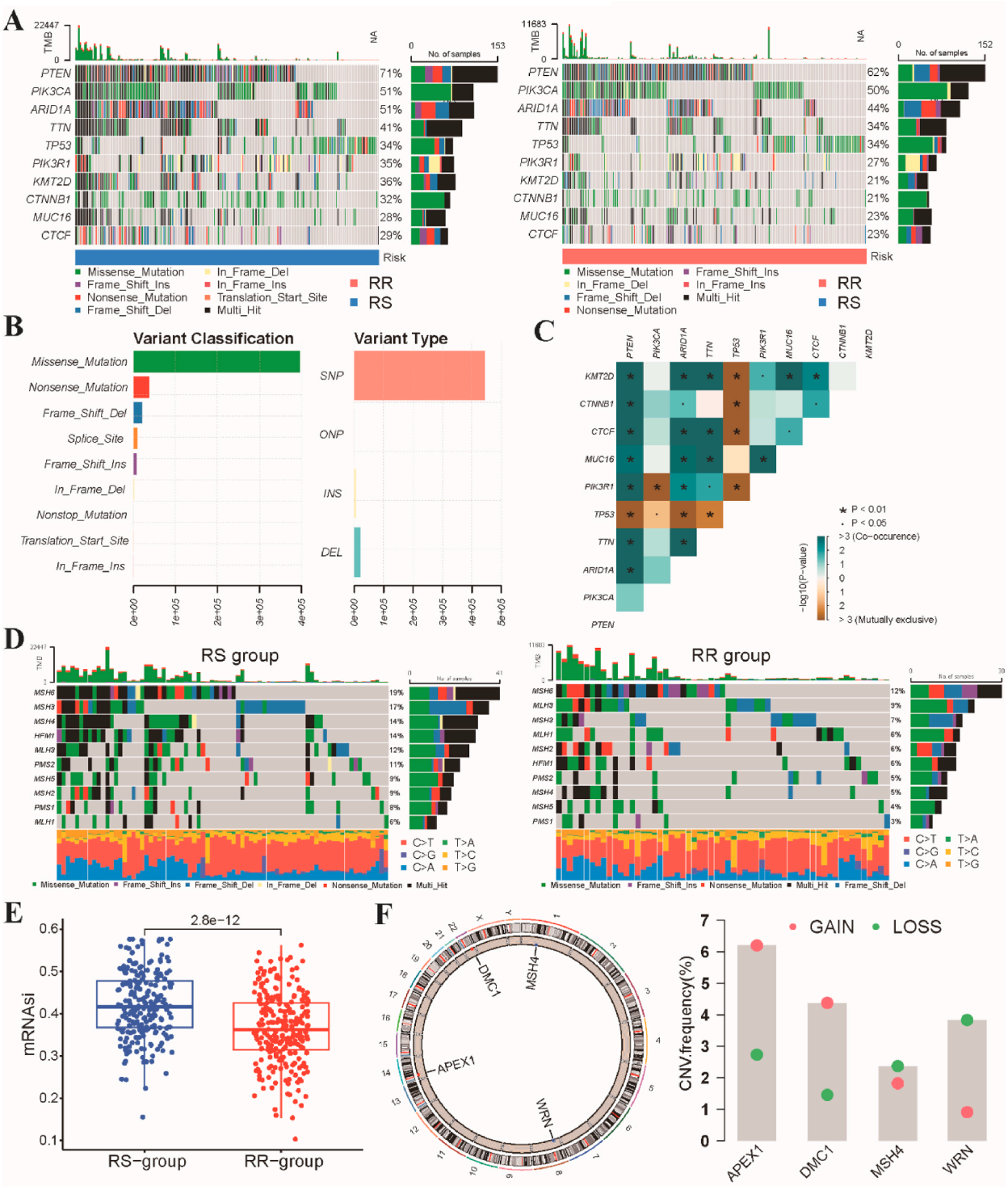

Fig. 3. Landscape of tumor mutational profile between RS and RR groups in the TCGA-UCEC dataset. **(A)** Waterfall plots were used to visualize the top 10 genes that were frequently mutated in both the RS and RR groups. (B) The most prevalent type of mutation in the TCGA-UCEC dataset was missense mutations, specifically single nucleotide polymorphisms. **(C)** A triangular matrix was utilized to present the mutually exclusive and co-occurring gene pairs. **(D)** Waterfall plots were employed to display the top 10 frequently mutated mismatch repair genes in the RS and RR groups. **(E)** The mRNAsi scores were compared between the RS group and the RR group to assess differences in stemness index. **(F)** The chromosomal location of CNV impacting the four repair-related genes was depicted across the 23 chromosomes. The column heights in the visualization indicate the proportions of gain or loss variations observed for each gene. *p < 0.05, **p < 0.01.

homologous DNA end joining (NHEJ), and various DNA single-strand break repair pathways (Fig. 4A). To further elucidate the relationship between the expression of the four genes comprising the radiosensitivity signature and the major pathways involved in DNA damage repair in UCEC, we performed a comprehensive analysis (Fig. 4B). Moreover, we used GSEA to examine and compare the variations in pathway enrichment between the RS and RR groups. It is worth mentioning that the RS group demonstrated a significant enrichment in biological processes closely associated with the detection of sister chromatid segregation and mitotic nuclear division. In contrast, the RR group exhibited a distinct enrichment in pathways related to the detection of chemical stimuli and chemical stimuli

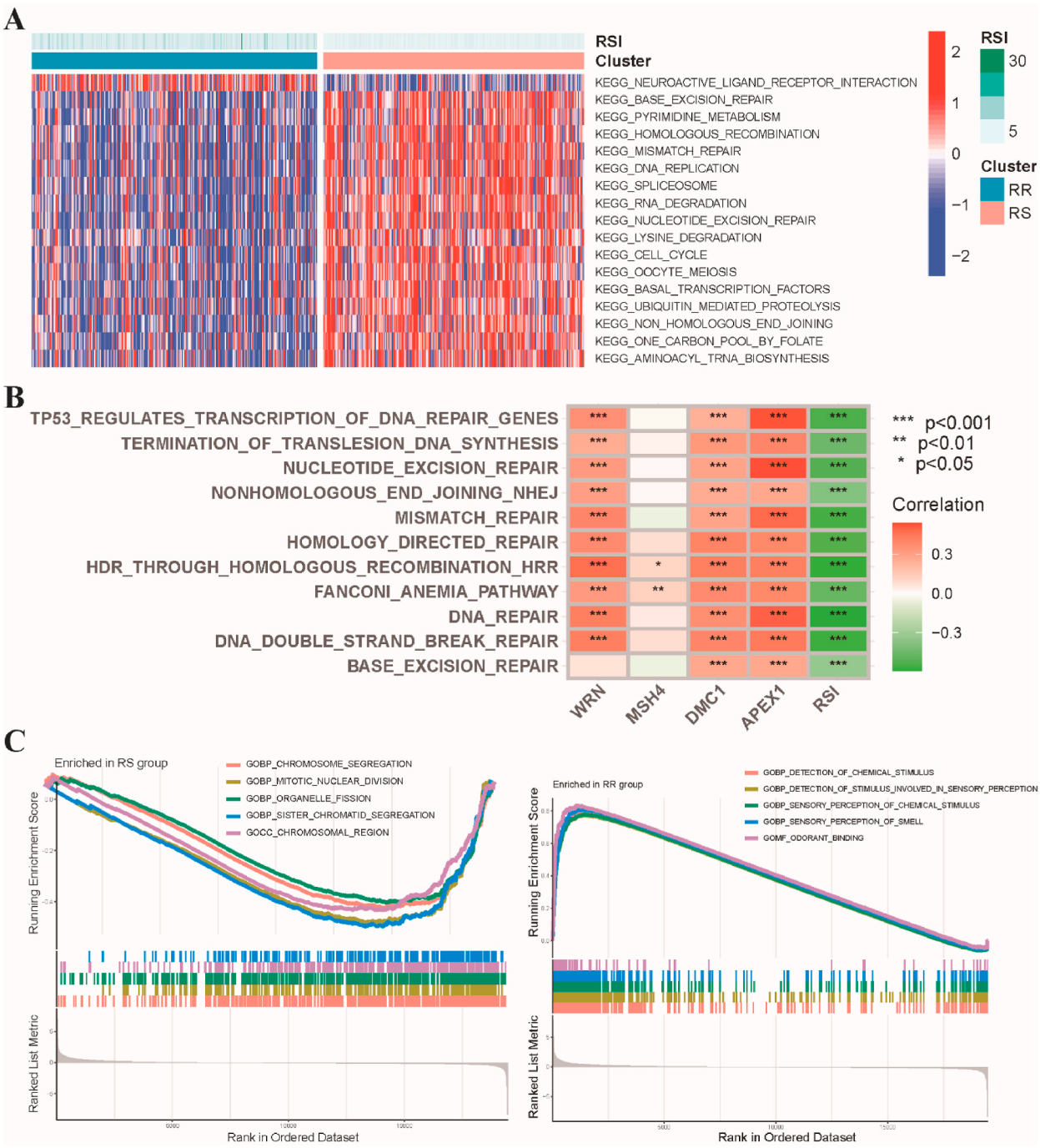

Fig. 4. Functional enrichment analysis of the radiosensitivity signature in UCEC. (A) Evaluation of pathway activity differences between RS and RR groups using GSVA. Pathway activities were scored per sample. **(B)** Correlation analysis between the expression levels of the four genes comprising the radiosensitivity signature and hallmark DNA damage repair pathways. **(C)** GSEA was conducted to confirm the biological functions associated with the RS and RR groups in the TCGA cohort. *p < 0.05, **p < 0.01, ***p < 0.001.

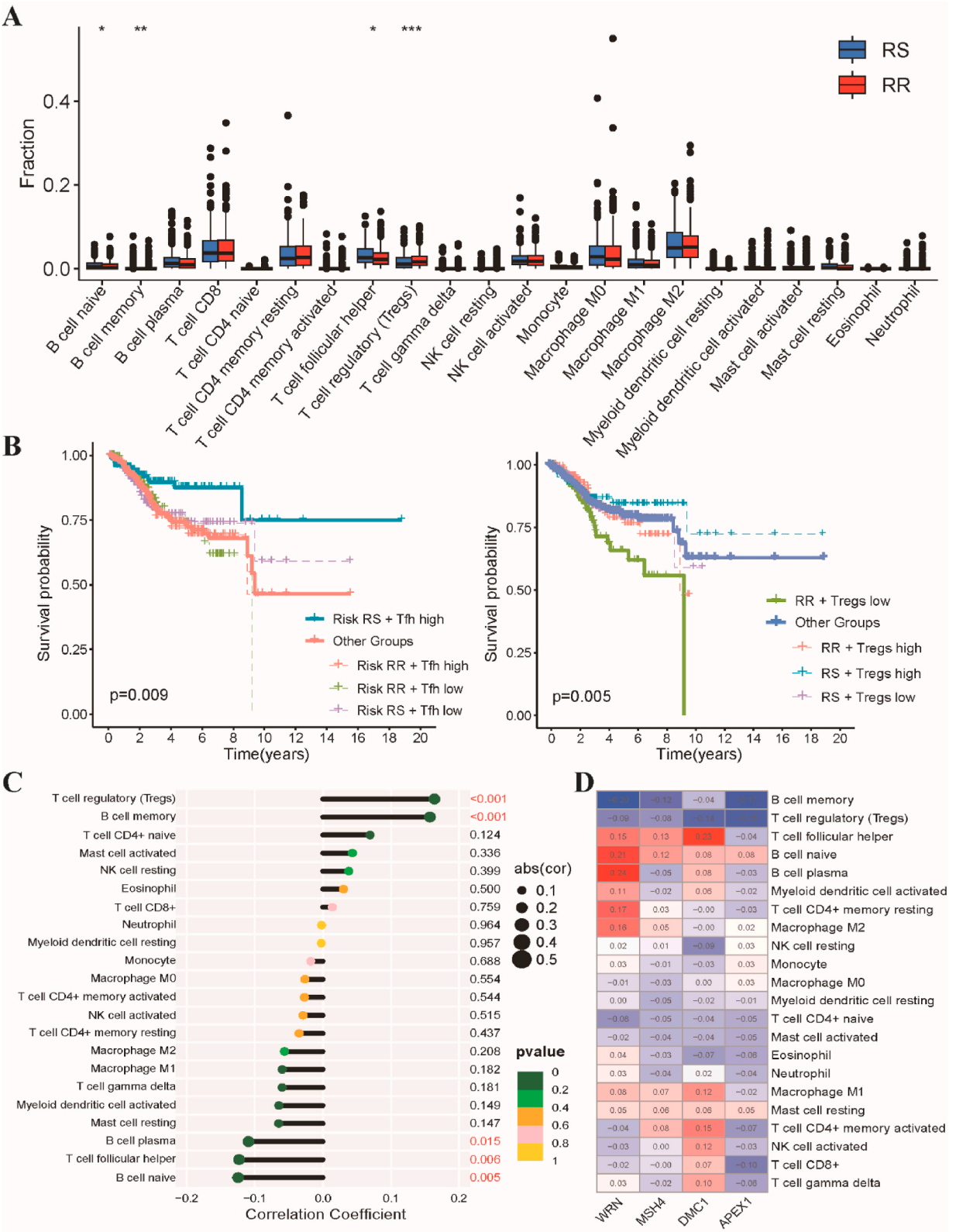

(caption on next page)

Fig. 5. Analysis of immune infiltrating cell profiles in RS and RR groups. (A) Comparative analysis of the proportions of 22 immune-infiltrating cells between the RS and RR groups. **(B)** Kaplan-Meier survival curves depicting OS in combination of immune cell proportions and radiosensitivity subgroups. **(C)** Investigation of the potential associations between immune cell populations and the radiosensitivity index. **(D)** Examination of the correlation between immune cells and the four genes included in the radiosensitivity index. *p < 0.05, **p < 0.01, ***p < 0.001.

involved in sensory perception (Fig. 4C). These findings provide valuable insights into the molecular mechanisms underlying the radiosensitivity signature in UCEC, highlighting the crucial role of DNA damage repair pathways and their potential implications in therapeutic response.

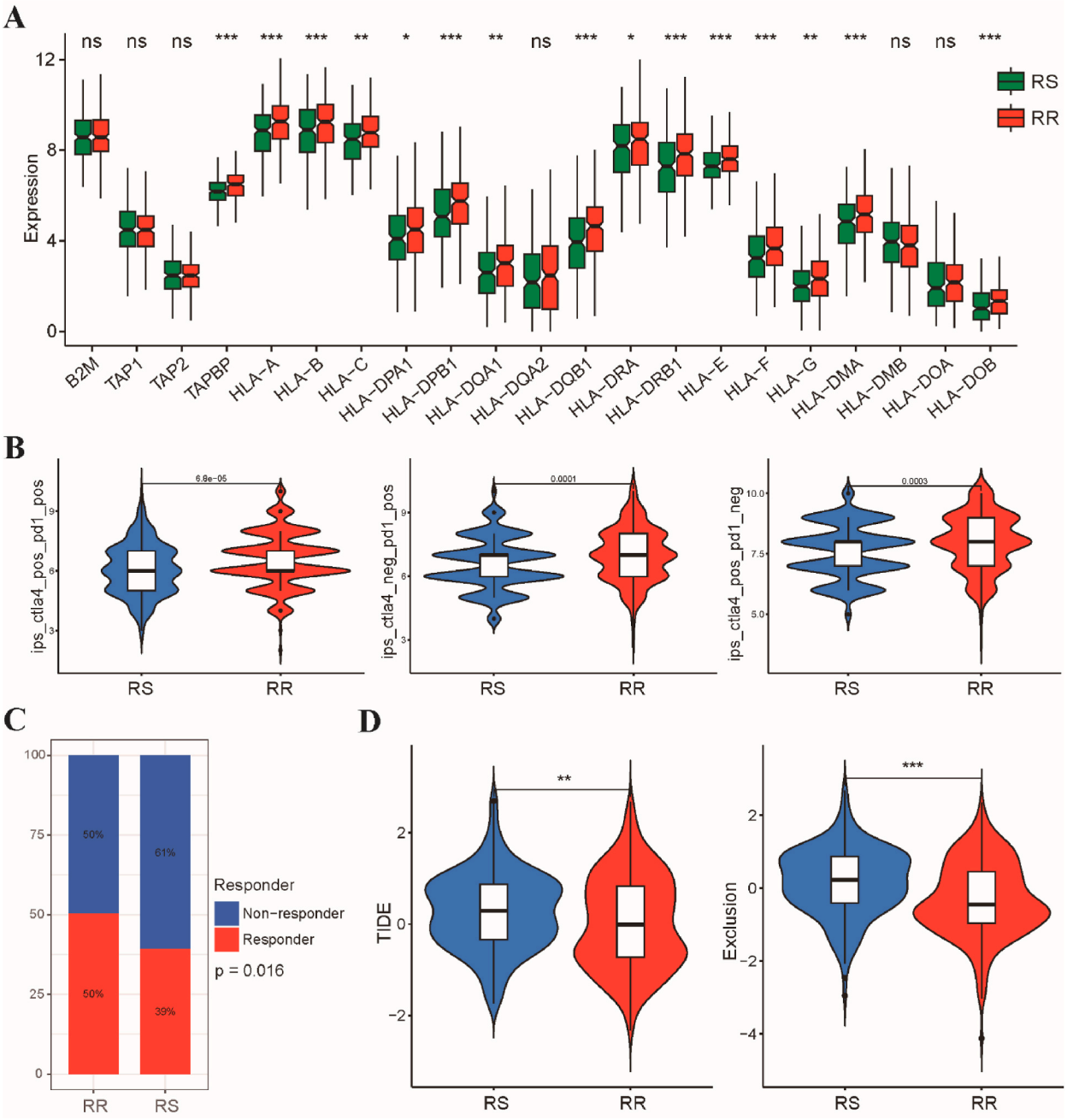

Fig. 6. Assessment of immunotherapy sensitivity in the TCGA-UCEC dataset between RS and RR group. (A) Association between the radiosensitivity signature and the expression levels of HLA-related genes in UCEC. **(B)** Violin plots illustrating the IPS values for CTLA-4 and PD-1 inhibitors in the RS and RR groups. **(C)** Stacked histogram displaying the distribution of responder and non-responder patients between two groups. **(D)** Calculation and comparison of TIDE scores and T-cell exclusion scores between the RS and RR groups.

3.5. Exploring the relationship between radiosensitivity signature and immune infiltration

In recent years, numerous studies have emphasized the crucial role of the tumor immune microenvironment in influencing the response to radiotherapy [26–30]. To further explore the correlation between the radiosensitivity signature and the status of tumor immune infiltration, we employed the CIBERSORT algorithm to evaluate the differences in the immune landscape between two groups. The CIBERSORT analysis provided additional insights into the immune cell composition of the RS and RR groups. Specifically, the RS group exhibited higher proportions of naïve B cells and follicular helper T (Tfh) cells, indicating a potentially enhanced immune response. In contrast, regulatory T cells (Tregs) and memory B cells were found to be more abundant in the RR group, suggesting a potential immunosuppressive environment (Fig. 5A). We proceeded to categorize the patients into four subgroups by considering a combination of immune cell proportions and radiosensitivity subgroup. Notably, the RS-Tfh-high subgroup demonstrated a significantly superior OS rate when compared to the remaining subgroups. Conversely, the RR-Tregs-low subgroup exhibited a significantly poorer OS rate in comparison to the other subgroups (Fig. 5B). Correlation analyses further supported these observations, revealing a significant negative correlation between the radiosensitivity index and tumor immune cell populations (Fig. 5C). Additionally, we investigated the associations between the expression levels of the 4-gene radiosensitivity index and the presence of 22 immune cells in UCEC (Fig. 5D). In addition, our analysis utilized multiple algorithms, including TIMER, QUANTISEQ, EPIC, and XCELL, to estimate the relationship between immune cells and the radiosensitivity index. Remarkably, we found a positive correlation between the radiosensitivity index and the regulatory T cells (Fig. S3B), further supporting the notion that immune infiltration may play a role in radiosensitivity.

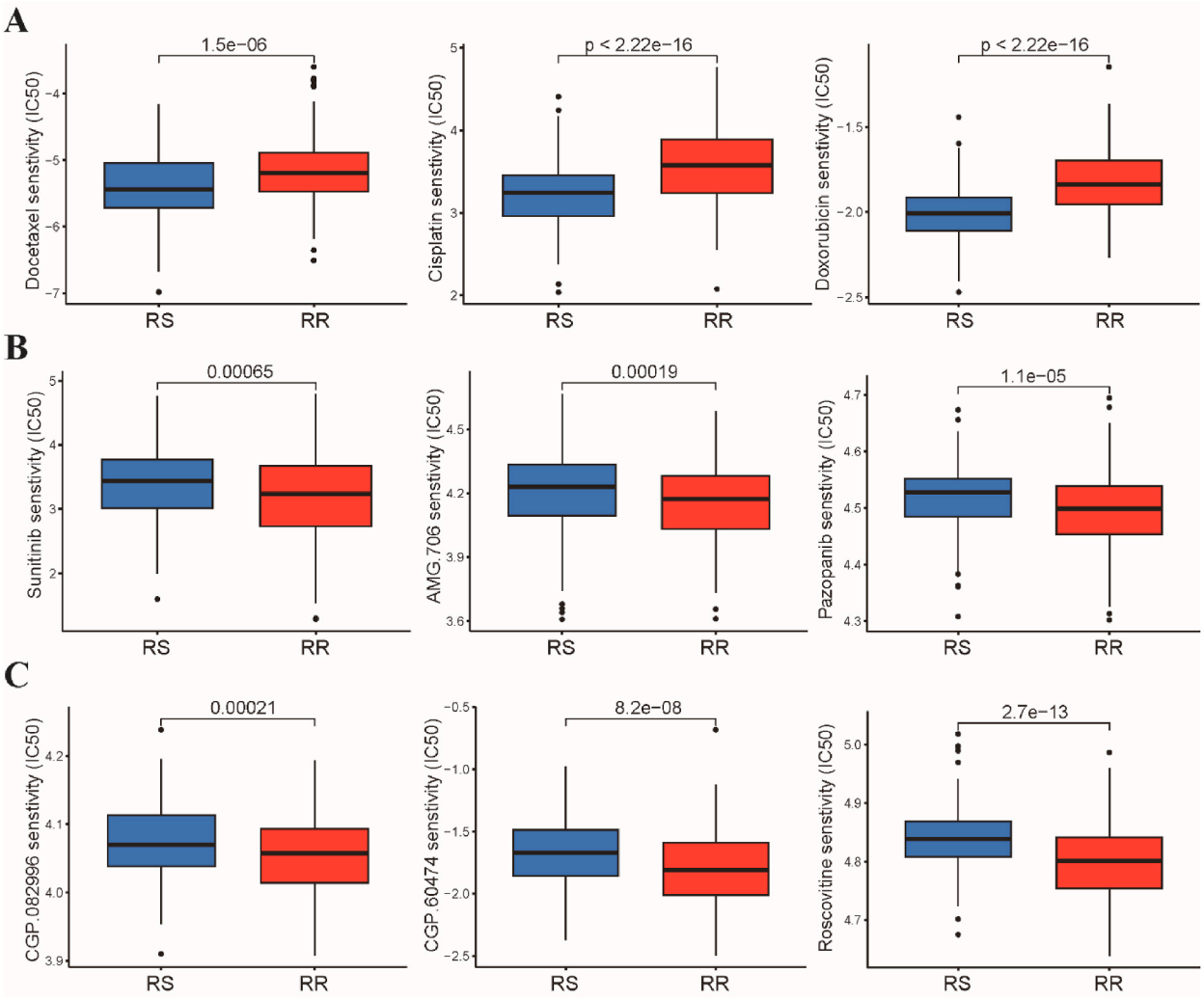

Fig. 7. Evaluation of drug sensitivity between these two radiosensitivity subtypes in TCGA-UCEC dataset. **(A)** Comparison of response to chemotherapy drugs, including docetaxel, cisplatin, and doxorubicin, between the RS group and the RR group. **(B)** Analysis of the IC50 values of three VEGFR inhibitors in the RS group and the RR group. **(C)** Assessment of the IC50 values of CDK inhibitors in both the RS group and the RR group.

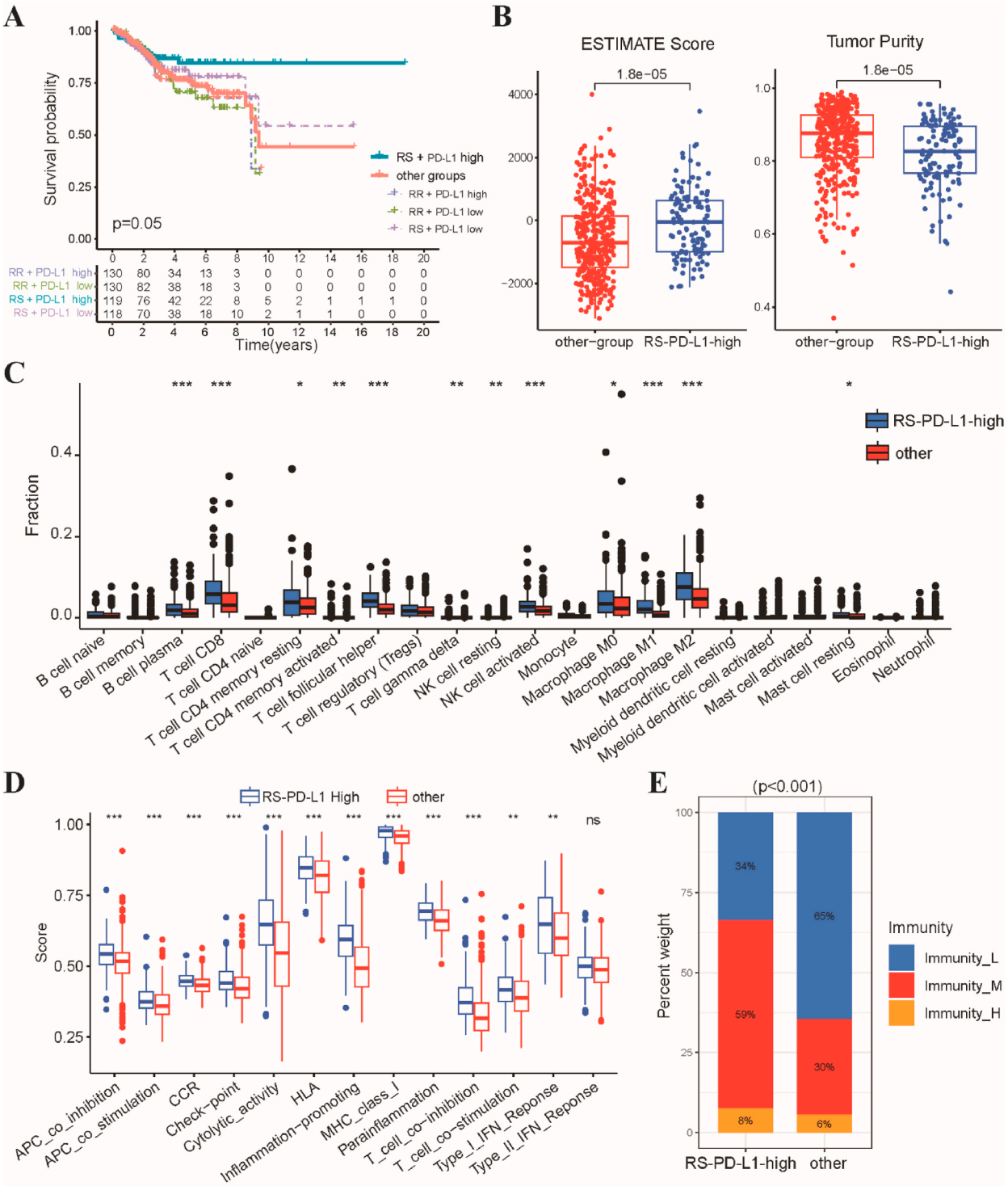

Fig. 8. Analysis of relationship between the radiosensitivity signature and PD-L1 expression. **(A)** Kaplan-Meier survival curves depicting OS in the RS-PD-L1-high subgroup compared to other subgroups. **(B)** Scatter plot comparing the levels of infiltration for estimate scores and tumor purity between the RS-PD-L1-high subgroup and the other subgroup. **(C)** Comparison of the proportions of 22 immune-infiltrating cells between the RS-PD-L1-high subgroup and the other subgroup. **(D)** Boxplots showed that RS-PD-L1-high subgroup exhibited higher enrichment scores in representative immune-related pathways. **(E)** Stacked histogram illustrating the proportions of high-immunity, middle-immunity, and low-immunity patients within the RS-PD-L1-high subgroup and the other subgroup. *p < 0.05, **p < 0.01, ***p < 0.001.

3.6. Correlation between radiosensitivity signature and immunotherapy sensitivity

Studies have shown that HLA gene expression significantly impacts the activation of antitumor immunity and patient response to immunotherapy [31,32]. In order to elucidate the potential mechanisms underlying the radiosensitivity signature and the efficacy of immunotherapy. We conducted further investigation to explore the differential expression of 21 genes associated with human leukocyte antigen class I and II (HLA-I/II) between the RS and RR groups. Our analysis revealed that a majority of HLA-I/II-related genes, such as HLA-A, HLA-B, HLA-E, HLA-F, HLA-DPA1, HLA-DPB1, HLA-DRB1, and HLA-DOB, exhibited elevated expression levels in the RR group (Fig. 6A), indicating that patients in RR group might be more sensitive to immunotherapy. Subsequently, we employed IPS and TIDE to further evaluate the immunotherapy sensitivity in patients with UCEC belonging to the RS and RR groups. As expected, the RR group demonstrated significantly higher IPS values compared to the RS group, as illustrated in Fig. 6B. This finding indicates a favorable response to both PD-1 and CTLA-4 inhibitors in the RR group. Furthermore, the TIDE algorithm corroborated our previous observations by demonstrating that patients in the RR group exhibited a better response to immunotherapy when compared to those in the RS group (Fig. 6C). The TIDE analysis revealed that the RR group had lower TIDE scores and T-cell exclusion scores in comparison to the RS group (Fig. 6D). These results further support the notion that patients in the RR group possess a more favorable immunotherapeutic response.

3.7. The relationship between the radiosensitivity signature and sensitivity to treatment

We conducted further investigations to examine the association between radiosensitivity signature and patient response to chemotherapy and targeted therapy. Utilizing the pRRophetic algorithm, our findings revealed that patients in the RS group exhibited higher sensitivity to first-line chemotherapy drugs, such as docetaxel, cisplatin, and doxorubicin, as evidenced by lower IC50 values compared to the RR group (Fig. 7A). The utilization of targeted therapy in the treatment of UCEC is a relatively recent development.

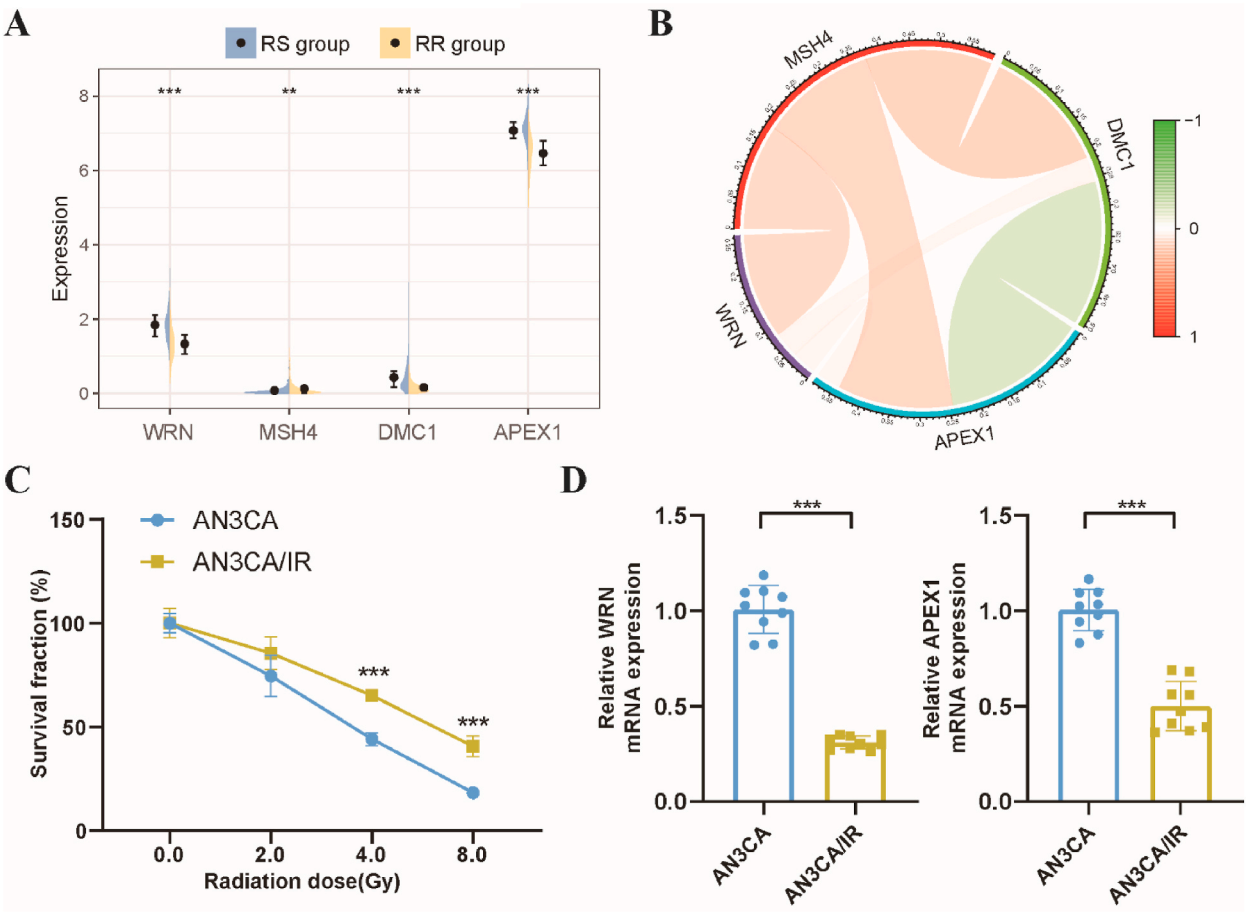

Fig. 9. Validation of the radiosensitivity genes in vitro experiment. **(A)** The expression levels of 4 radiosensitivity genes between the RS and RR groups in the boxplot. **(B)** The correlation analysis of 4 radiosensitivity genes. **(C)** The proliferative capacity of AN3CA and AN3CA/IR cells after radiation exposure was evaluated using the CCK8 assay. **(D)** The qRT-PCR was utilized to assess the expression levels of WRN and APEX1 in AN3CA and AN3CA/IR cells. $^{**}p < 0.01$, $^{***}p < 0.001$.

While a limited number of targeted therapy drugs are currently employed, and many more are being studied. Among these potential therapeutic targets, the vascular endothelial growth factor receptor (VEGFR) has garnered considerable attention due to its pivotal role in angiogenesis and the pathogenesis of UCEC [33]. Our results demonstrated that the RS group had higher IC50 values in comparison to the RR group, indicating that patients in the RR group may display higher sensitivity to VEGFR Kinase inhibitors (Fig. 7B). Additionally, given the involvement of cyclin-dependent kinases (CDKs) in promoting the occurrence and development of UCEC, CDK inhibitors have emerged as a promising therapeutic approach [34,35]. Through our analysis, we estimated the IC50 values of CDK inhibitors and observed that they were significantly lower in patients belonging to the RR group (Fig. 7C). These findings suggested that CDK inhibitors may have the potential to re-sensitize the RR group to radiation therapy.

3.8. Exploring the relationship between the radiosensitivity signature and PD-L1 expression

In light of the growing importance of PD-1/PD-L1 in UCEC patients, we aimed to explore the relationship between the radiosensitivity signature and the expression levels of CD274 mRNA, which encodes PD-L1. Our analysis revealed no significant difference in PD-1 expression between the RS and RR groups (Fig. S4A). We further categorized the patients into four subgroups based on a combination of PD-L1 levels (PD-L1-high vs. PD-L1-low) and their radiosensitivity status (RR vs. RS). Interestingly, the subgroup characterized by high PD-L1 expression and radiosensitivity (RS-PD-L1-high group) exhibited a significantly better OS rate compared to the other subgroups (Fig. 8A). Using the ESTIMATE algorithm, the analysis revealed that the RS-PD-L1-high subgroup had significantly higher estimate scores compared to the other subgroups. Conversely, tumor purity was found to be decreased in the RS-PD-L1-high subgroup (Fig. 8B). Next, utilizing the CIBERSORT algorithm, the RS-PD-L1-high subgroup displayed higher proportions of major immune cell types, including CD8 T cells, plasma B cells, follicular T helper cells, NK cells, and macrophages (Fig. 8C). Furthermore, we employed the ssGSEA algorithm based on 29 immune gene sets. Our analysis revealed that the RS-PD-L1-high subgroup was enriched in several immune-related pathways, such as T-cell costimulation/inhibition, antigen-presenting cell costimulation/inhibition, and type I/II interferon response (Fig. 8D). Notably, we categorized patients into high-immunity, middle-immunity, and low-immunity subgroups based on their ssGSEA scores. Consistent with our previous findings, the RS-PD-L1-high subgroup predominantly consisted of patients with middle immunity and high immunity (Fig. 8E). The IPS and TIDE algorithms showed that the RS-PD-L1-high subgroup had a more favorable immunotherapeutic response (Figs. S4B–C). These findings provide valuable insights into the association between immune activation, PD-L1 expression and immunotherapeutic response in the context of radiosensitivity.

3.9. Validation of the radiosensitivity genes in vitro experiment

Finally, we conducted in vitro experiments to validate the expression of radiosensitivity genes. Fig. 9A displays the expression levels of four genes in the radiosensitivity signature between the RS and RR groups. Correlation analysis was performed for the four DNA repair-related genes (Fig. 9B). Subsequently, we utilized non-radioresistant AN3CA cells and radioresistant AN3CA/IR cells to verify the expression of these four genes. The radioresistant ability of AN3CA/IR cells was assessed using the Cell Counting Kit-8 (CCK-8) assay. Compared to AN3CA cells, the viability of AN3CA/IR cells exhibited an increase upon exposure to radiation doses of 2, 4, and 8 Gy, indicating the radioresistant feature of AN3CA/IR cells (Fig. 9C). The expression levels of WRN and APEX1 were higher in AN3CA cells than in radioresistant AN3CA/IR cells, consistent with our bioinformatics analysis (Fig. 9D). However, no statistically significant differences were observed in the expression levels of MSH4 and DMC1 between the RS and RR groups.

4. Discussion

For several decades, radiotherapy has been the established adjuvant treatment for women with high-risk UCEC [36]. In recent years, the implementation of high-throughput molecular profiling has led to a risk-based approach in radiotherapy for UCEC patients [37]. The identification of molecular subgroups within UCEC has allowed for a more robust classification system with prognostic or predictive implications [38]. Importantly, the molecular classification not only possesses the capability to predict the response to radiotherapy but also enables the identification of distinct molecular targets that can be effectively addressed using currently available therapeutic agents. In our study, we aimed to develop a radiosensitivity signature that could accurately predict the response to radiotherapy in UCEC patients. We further analysis the biological enrichment, clinical differences and immune landscapes between patients classified as RS and RR groups based on radiosensitivity index. Moreover, our findings revealed that both the radiosensitivity signature and PD-L1 expression status held promise as predictive factors for the response to radiotherapy.

The identification of key gene signatures has been a significant challenge in the field of radiosensitivity, as it serves as a prerequisite for developing effective predictive models [39]. To address this challenge, genome-wide screening approaches have been employed, leading to the discovery of specific gene sets associated with radiosensitivity. One notable example is the radiosensitivity signature comprising 31 genes, which was developed based on profiling the NCI-60 cell line panel. This signature has been validated in various tumor types, including breast cancer, lower grade glioma, and pancreatic cancer [40]. Additionally, a ten-gene signature for cellular radiosensitivity has been established to predict the sensitivity of 48 cancer cell lines to radiation. This radiosensitivity index has undergone independent validation across multiple cancer types [41]. However, is crucial to acknowledge that the term “radiosensitivity” can encompass different definitions. Within the realm of clinical practice, radiosensitivity is defined by at least two criteria. Firstly, when both the RS and RR groups undergo radiotherapy, the RS group should exhibit significantly greater survival benefits compared to the RR group. Secondly, in the absence of radiotherapy, the survival rate of the RS group should not surpass that of the RR

group [39]. In our study, we found that the RS group demonstrated superior OS and DSS rates compared to the RR group among UCEC patients who received radiotherapy. Importantly, this difference in survival outcomes was not observed among patients who did not undergo radiotherapy. These findings provide robust evidence supporting the validity of the radiosensitivity model as a predictive marker for UCEC patients.

UCEC has long been acknowledged as a cancer with diverse histological and molecular characteristics that hold potential as predictive biomarkers [42]. In our study, we observed frequent mutations in PTEN, PIK3CA, ARID1A, and P53, indicating their significance in UCEC. Notably, UCEC exhibits a higher frequency of mutations in the PTEN/PI3K/AKT pathway compared to other tumor types, presenting translational opportunities for targeted therapeutic interventions. TCGA has played a vital role in identifying these molecular subsets by conducting comprehensive molecular analyses on 373 endometrial cancers [43]. This analysis revealed four distinct subsets with varying prognoses: POLE ultra-mutated, microsatellite instability hypermutated, copy number low, and copy number high. In our study, we found that the RS group predominantly consisted of the POLE ultra-mutated subset. The mutational status of POLE has been validated as an independent prognostic factor for UCEC patients, with those harboring somatic POLE mutations demonstrating a favorable prognosis [44]. Additionally, POLE mutations have been shown to regulate cytokine secretion, thereby influencing immune responses. This may partially explain why patients in the RS group exhibited a higher sensitivity to radiotherapy. Consequently, one of the objectives of our study was to establish a potential relationship between POLE mutations and radiosensitivity.

The DNA repair pathway plays a critical role in maintaining genomic stability and repairing DNA damage induced by radiation therapy [45]. UCEC exhibit heterogeneity in their DNA repair capacity, which can impact their response to radiotherapy. Our study showed that the RS group exhibited significant enrichment in DNA damage repair pathways. Dysregulation of the HR pathway can result in impaired DNA repair and increased radiosensitivity [46]. In addition to the HR pathway, other DNA repair pathways, such as NHEJ and BER, also contribute to the repair of radiation-induced DNA damage [47]. Furthermore, the relationship between DNA repair pathway, immune infiltration, and radiosensitivity in UCEC is of great interest. The results of our study reveal an intriguing relationship between immune cell proportions, radiosensitivity, and OS rates in UCEC patients. The RS-Tfh-high subgroup demonstrated a significantly superior OS rate compared to the other subgroups. This finding suggests that a higher proportion of Tfh cells, which are crucial for promoting B cell activation and antibody production. Conversely, the RR-Tregs-low subgroup exhibited a significantly poorer OS rate compared to the other subgroups. Our findings suggest that an immunosuppressive microenvironment characterized by increased Tregs may contribute to radiation resistance and poorer survival outcomes in UCEC patients. This observation presents a potential therapeutic opportunity to exploit the inherent immunoreactivity of these tumors by priming the immune system for immunotherapy, potentially enhancing its efficacy.

Immunotherapy, harnessing the body's intrinsic immune response against tumors, has emerged as a promising treatment option, with several immune checkpoint inhibitors approved for various cancers, including UCEC [48,49]. However, responsiveness to these therapies remains variable. Combination strategies with immune checkpoint inhibitors and other modalities, such as chemotherapy or radiotherapy, are actively investigated in UCEC [50]. Notably, our study suggests a differential response to immunotherapy, with patients in the RR group demonstrating a more favorable response compared to the RS group. This finding may be attributed to the presence of distinct immune cell subsets. The higher Immunophenotype Score (IPS) and improved immunotherapy response observed in the RR group could be explained by the presence of immunosuppressive cell subsets, such as Tregs. Inhibiting immune checkpoints like PD-1 and CTLA-4 may overcome the immunosuppressive effects of Tregs, potentially enhancing immunotherapy efficacy. Therefore, targeting Tregs or modulating the immunosuppressive microenvironment may hold promise for improving immunotherapy response, particularly in the RR group. These findings pave the way for personalized immunotherapy strategies in UCEC, offering a more tailored approach to optimize treatment outcomes.

PD-L1 overexpression has been observed in various human malignancies and has been associated with a poor prognosis and resistance to anticancer therapies [51,52]. Therefore, identifying key targets that can inhibit PD-L1 expression and subsequently enhance T-cell function has become a significant focus of research in the field of cancer immunotherapy. Interestingly, when we categorized the patients into subgroups based on a combination of PD-L1 levels and radiosensitivity status, we made some intriguing observations. We found that the RS-PD-L1-high subgroup had significantly higher immune cell infiltration, immune-related pathways and better OS rate compared to the other subgroups. Consistent with our previous results, the RS-PD-L1-high subgroup predominantly consisted of patients with middle immunity and high immunity. These results suggested that the RS-PD-L1-high subgroup may have a more activated and diverse immune response, which could contribute to their improved prognosis. Our study provides valuable insights for the development of personalized immunotherapy approaches in UCEC. Further studies are needed to validate these findings and explore the underlying mechanisms driving the association between immune activation, PD-L1 expression, and radiosensitivity in UCEC.

Several limitations should be acknowledged in our study. Firstly, the retrospective nature of our study, utilizing publicly available TCGA cohorts, raises the need for validation in a prospective cohort to ensure the robustness and generalizability of our findings. Moreover, the use of two cell lines for validation is a limited approach. In future studies, it would be important to validate our findings using clinical specimens or additional cell lines. Secondly, it is worth noting that while previous studies commonly employed immunohistochemistry as a means to assess PD-L1 expression, we chose to utilize CD274 mRNA expression as a surrogate marker. Lastly, Although the radiosensitivity index identified in this study was predictive of patient prognosis, only two of the four genes included in the index were validated in in vitro experiments. This suggests that the in vitro cell culture model used in this study does not fully recapitulate the complex tumor microenvironment of patients receiving radiotherapy. Future studies using more clinically relevant models, such as patient-derived xenografts, are needed to confirm the findings of this study and to identify additional DNA repair-related biomarkers that could be used to predict patient prognosis and response to radiotherapy.

5. Conclusion

In summary, our study successfully developed a signature based on DNA repair-related genes that can accurately identify UCEC patients who are likely to benefit from radiotherapy. We observed significant enrichment of DNA damage repair pathways in the signature-defined RS group. Specifically, the RS group demonstrated higher proportions of naïve B cells and follicular helper T cells, while Tregs and memory B cells were more abundant in the RR group. Furthermore, patients classified into the RS-PD-L1-high subgroup exhibited enriched in immune-related pathways and increased sensitivity to immunotherapy, which is likely to contribute to their improved prognosis.

Funding statement

This work was supported by grants from Natural Science Foundation of Fujian Province (Grant No. 2021J01247) and Doctoral Project of the Second Affiliated Hospital of Fujian Medical University (Grant No. BS202110).

Data availability statement

The datasets supporting our researches are presented in the article.

Ethics approval and consent to participate

Not applicable.

CRediT authorship contribution statement

Hainan Yang: Conceptualization, Data curation, Formal analysis, Methodology, Software, Validation, Visualization, Writing – original draft, Writing – review & editing. **Yanru Qiu:** Data curation, Methodology, Resources, Software, Validation, Visualization. **Junjun Chen:** Methodology, Resources, Software, Validation, Visualization. **Jinzhi Lai:** Conceptualization, Data curation, Formal analysis, Funding acquisition, Supervision, Writing – review & editing, Project administration.

Declaration of competing interest

The authors declare that they have no known competing financial interests or personal relationships that could have appeared to influence the work reported in this paper.

Appendix A. Supplementary data

Supplementary data to this article can be found online at https://doi.org/10.1016/j.heliyon.2024.e29401.

References

[1] R.L. Siegel, K.D. Miller, H.E. Fuchs, A. Jemal, Cancer statistics, 2022, CA A Cancer J. Clin. 72 (2022) 7–33.
[2] H. Sung, J. Ferlay, R.L. Siegel, M. Laversanne, I. Soerjomataram, A. Jemal, F. Bray, Global cancer statistics 2020: GLOBOCAN estimates of incidence and mortality worldwide for 36 cancers in 185 countries, CA A Cancer J. Clin. 71 (2021) 209–249.
[3] R. Zheng, S. Zhang, H. Zeng, S. Wang, K. Sun, R. Chen, L. Li, W. Wei, J. He, Cancer incidence and mortality in China, 2016, Journal of the National Cancer Center 2 (2022) 1–9.
[4] A. van den Heerik, N. Horeweg, S.M. de Boer, T. Bosse, C.L. Creutzberg, Adjuvant therapy for endometrial cancer in the era of molecular classification: radiotherapy, chemoradiation and novel targets for therapy, Int. J. Gynecol. Cancer : official journal of the International Gynecological Cancer Society 31 (2021) 594–604.
[5] R.A. Brooks, G.F. Fleming, R.R. Lastra, N.K. Lee, J.W. Moroney, C.H. Son, K. Tatebe, J.L. Veneris, Current recommendations and recent progress in endometrial cancer, CA A Cancer J. Clin. 69 (2019) 258–279.
[6] M.A. Sorolla, E. Parisi, A. Sorolla, Determinants of sensitivity to radiotherapy in endometrial cancer, Cancers 12 (2020).
[7] Z. Nikitaki, A. Velalopoulou, V. Zanni, I. Tremi, S. Havaki, M. Kokkoris, V.G. Gorgoulis, C. Koumenis, A.G. Georgakilas, Key biological mechanisms involved in high-LET radiation therapies with a focus on DNA damage and repair, Expet Rev. Mol. Med. 24 (2022) e15.
[8] F. Sadoughi, L. Mirsafaei, P.M. Dana, J. Hallajzadeh, Z. Asemi, M.A. Mansournia, M. Montazer, M. Hosseinpour, B. Yousefi, The role of DNA damage response in chemo- and radio-resistance of cancer cells: can DDR inhibitors sole the problem? DNA Repair 101 (2021) 103074.
[9] I. Larionova, M. Rakina, E. Ivanyuk, Y. Trushchuk, A. Chernyshova, E. Denisov, Radiotherapy resistance: identifying universal biomarkers for various human cancers, J. Cancer Res. Clin. Oncol. 148 (2022) 1015–1031.
[10] T.M. Malta, A. Sokolov, A.J. Gentles, T. Burzykowski, L. Poisson, J.N. Weinstein, B. Kamińska, J. Huelsken, L. Omberg, O. Gevaert, A. Colaprico, P. Czerwińska, S. Mazurek, L. Mishra, H. Heyn, A. Krasnitz, A.K. Godwin, A.J. Lazar, J.M. Stuart, K.A. Hoadley, P.W. Laird, H. Noushmehr, M. Wiznerowicz, Machine learning identifies stemness features associated with oncogenic dedifferentiation, Cell 173 (2018) 338, 54.e15.
[11] H. Zhang, P. Meltzer, S. Davis, RCircos: an R package for Circos 2D track plots, BMC Bioinf. 14 (2013) 244.
[12] S. Hanzelmann, R. Castelo, J. Guinney, GSVA: gene set variation analysis for microarray and RNA-seq data, BMC Bioinf. 14 (2013) 7.
[13] M. Kanehisa, Y. Sato, M. Kawashima, KEGG mapping tools for uncovering hidden features in biological data, Protein Sci. : a publication of the Protein Society 31 (2022) 47–53.

[14] B. Chen, M.S. Khodadoust, C.L. Liu, A.M. Newman, A.A. Alizadeh, Profiling tumor infiltrating immune cells with CIBERSORT, Methods Mol. Biol. 1711 (2018) 243–259.
[15] A.M. Newman, C.L. Liu, M.R. Green, A.J. Gentles, W. Feng, Y. Xu, C.D. Hoang, M. Diehn, A.A. Alizadeh, Robust enumeration of cell subsets from tissue expression profiles, Nat. Methods 12 (2015) 453–457.
[16] G. Bindea, B. Mlecnik, M. Tosolini, A. Kirilovsky, M. Waldner, A.C. Obenauf, H. Angell, T. Fredriksen, L. Lafontaine, A. Berger, P. Bruneval, W.H. Fridman, C. Becker, F. Pagès, M.R. Speicher, Z. Trajanoski, J. Galon, Spatiotemporal dynamics of intratumoral immune cells reveal the immune landscape in human cancer, Immunity 39 (2013) 782–795.
[17] K. Yoshihara, M. Shahmoradgoli, E. Martínez, R. Vegesna, H. Kim, W. Torres-Garcia, V. Treviño, H. Shen, P.W. Laird, D.A. Levine, S.L. Carter, G. Getz, K. Stemke-Hale, G.B. Mills, R.G. Verhaak, Inferring tumour purity and stromal and immune cell admixture from expression data, Nat. Commun. 4 (2013) 2612.
[18] T. Li, J. Fu, Z. Zeng, D. Cohen, J. Li, Q. Chen, B. Li, X.S. Liu, TIMER2.0 for analysis of tumor-infiltrating immune cells, Nucleic Acids Res. 48 (2020) W509, w14.
[19] F. Finotello, C. Mayer, C. Plattner, G. Laschober, D. Rieder, H. Hackl, A. Krogsdam, Z. Loncova, W. Posch, D. Wilflingseder, S. Sopper, M. Ijsselsteijn, T. P. Brouwer, D. Johnson, Y. Xu, Y. Wang, M.E. Sanders, M.V. Estrada, P. Ericsson-Gonzalez, P. Charoentong, J. Balko, N. de Miranda, Z. Trajanoski, Molecular and pharmacological modulators of the tumor immune contexture revealed by deconvolution of RNA-seq data, Genome Med. 11 (2019) 34.
[20] J. Racle, D. Gfeller, EPIC: a tool to estimate the proportions of different cell types from bulk gene expression data, Methods Mol. Biol. 2120 (2020) 233–248.
[21] D. Aran, Z. Hu, A.J. Butte, xCell: digitally portraying the tissue cellular heterogeneity landscape, Genome Biol. 18 (2017) 220.
[22] W. Hugo, J.M. Zaretsky, L. Sun, C. Song, B.H. Moreno, S. Hu-Lieskovan, B. Berent-Maoz, J. Pang, B. Chmielowski, G. Cherry, E. Seja, S. Lomeli, X. Kong, M. C. Kelley, J.A. Sosman, D.B. Johnson, A. Ribas, R.S. Lo, Genomic and transcriptomic features of response to Anti-PD-1 therapy in metastatic melanoma, Cell 165 (2016) 35–44.
[23] P. Jiang, S. Gu, D. Pan, J. Fu, A. Sahu, X. Hu, Z. Li, N. Traugh, X. Bu, B. Li, J. Liu, G.J. Freeman, M.A. Brown, K.W. Wucherpfennig, X.S. Liu, Signatures of T cell dysfunction and exclusion predict cancer immunotherapy response, Nat. Med. 24 (2018) 1550–1558.
[24] P. Geeleher, N. Cox, R. Huang, pRRophetic: an R package for prediction of clinical chemotherapeutic response from tumor gene expression levels, PLoS One 9 (2014) e107468.
[25] Z.R. Zhou, X.Y. Wang, X.L. Yu, X. Mei, X.X. Chen, Q.C. Hu, Z.Z. Yang, X.M. Guo, Building radiation-resistant model in triple-negative breast cancer to screen radioresistance-related molecular markers, Ann. Transl. Med. 8 (2020) 108.
[26] S. Taeb, M. Ashrafizadeh, A. Zarrabi, S. Rezapoor, A.E. Musa, B. Farhood, M. Najafi, Role of tumor microenvironment in cancer stem cells resistance to radiotherapy, Curr. Cancer Drug Targets 22 (2022) 18–30.
[27] J.H. Kaanders, K.I. Wijffels, H.A. Marres, A.S. Ljungkvist, L.A. Pop, F.J. van den Hoogen, P.C. de Wilde, J. Bussink, J.A. Raleigh, A.J. van der Kogel, Pimonidazole binding and tumor vascularity predict for treatment outcome in head and neck cancer, Cancer Res. 62 (2002) 7066–7074.
[28] T. Suwa, M. Kobayashi, J.M. Nam, H. Harada, Tumor microenvironment and radioresistance, Exp. Mol. Med. 53 (2021) 1029–1035.
[29] P.J. Cook, R. Thomas, P.J. Kingsley, F. Shimizu, D.C. Montrose, L.J. Marnett, V.S. Tabar, A.J. Dannenberg, R. Benezra, Cox-2-derived PGE2 induces Id1-dependent radiation resistance and self-renewal in experimental glioblastoma, Neuro Oncol. 18 (2016) 1379–1389.
[30] S. Andersen, T. Donnem, S. Al-Saad, K. Al-Shibli, L.T. Busund, R.M. Bremnes, Angiogenic markers show high prognostic impact on survival in marginally operable non-small cell lung cancer patients treated with adjuvant radiotherapy, J. Thorac. Oncol. : official publication of the International Association for the Study of Lung Cancer 4 (2009) 463–471.
[31] N. Jiang, Y. Yu, D. Wu, S. Wang, Y. Fang, H. Miao, P. Ma, H. Huang, M. Zhang, Y. Zhang, Y. Tang, N. Li, HLA and tumour immunology: immune escape, immunotherapy and immune-related adverse events, J. Cancer Res. Clin. Oncol. 149 (2023) 737–747.
[32] E. Schaafsma, C.M. Fugle, X. Wang, C. Cheng, Pan-cancer association of HLA gene expression with cancer prognosis and immunotherapy efficacy, Br. J. Cancer 125 (2021) 422–432.
[33] A.A. Berger, F. Dao, D.A. Levine, Angiogenesis in endometrial carcinoma: therapies and biomarkers, current options, and future perspectives, Gynecol. Oncol. 160 (2021) 844–850.
[34] G. Giannone, V. Tuninetti, E. Ghisoni, S. Genta, G. Scotto, G. Mittica, G. Valabrega, Role of cyclin-dependent kinase inhibitors in endometrial cancer, Int. J. Mol. Sci. 20 (2019).
[35] R.K. Singla, S. Behzad, J. Khan, C. Tsagkaris, R.K. Gautam, R. Goyal, H. Chopra, B. Shen, Natural kinase inhibitors for the treatment and management of endometrial/uterine cancer: preclinical to clinical studies, Front. Pharmacol. 13 (2022) 801733.
[36] M.M. Harkenrider, N. Abu-Rustum, K. Albuquerque, L. Bradfield, K. Bradley, E. Dolinar, C.M. Doll, M. Elshaikh, M.A. Frick, P.A. Gehrig, K. Han, L. Hathout, E. Jones, A. Klopp, F. Mourtada, G. Suneja, A.A. Wright, C. Yashar, B.A. Erickson, Radiation therapy for endometrial cancer: an American society for radiation oncology clinical practice guideline, Practical radiation oncology 13 (2023) 41–65.
[37] A. León-Castillo, S.M. de Boer, M.E. Powell, L.R. Mileshkin, H.J. Mackay, A. Leary, H.W. Nijman, N. Singh, P.M. Pollock, P. Bessette, A. Fyles, C. Haie-Meder, V. Smit, R.J. Edmondson, H. Putter, H.C. Kitchener, E.J. Crosbie, M. de Bruyn, R.A. Nout, N. Horeweg, C.L. Creutzberg, T. Bosse, Molecular classification of the PORTEC-3 trial for high-risk endometrial cancer: impact on prognosis and benefit from adjuvant therapy, J. Clin. Oncol. : official journal of the American Society of Clinical Oncology 38 (2020) 3388–3397.
[38] D.W. Bell, L.H. Ellenson, Molecular genetics of endometrial carcinoma, Annual review of pathology 14 (2019) 339–367.
[39] Z. Du, X. Zhang, Z. Tang, More evidence for prediction model of radiosensitivity, Biosci. Rep. 41 (2021).
[40] H.S. Kim, S.C. Kim, S.J. Kim, C.H. Park, H.C. Jeung, Y.B. Kim, J.B. Ahn, H.C. Chung, S.Y. Rha, Identification of a radiosensitivity signature using integrative metaanalysis of published microarray data for NCI-60 cancer cells, BMC Genom. 13 (2012) 348.
[41] S. Eschrich, H. Zhang, H. Zhao, D. Boulware, J.H. Lee, G. Bloom, J.F. Torres-Roca, Systems biology modeling of the radiation sensitivity network: a biomarker discovery platform, Int. J. Radiat. Oncol. Biol. Phys. 75 (2009) 497–505.
[42] R. Wu, C. Wu, B. Zhu, J. Li, W. Zhao, Screening and validation of potential markers associated with uterine corpus endometrial carcinoma and polycystic ovary syndrome based on bioinformatics methods, Front. Mol. Biosci. 10 (2023) 1192313.
[43] C. Kandoth, N. Schultz, A.D. Cherniack, R. Akbani, Y. Liu, H. Shen, A.G. Robertson, I. Pashtan, R. Shen, C.C. Benz, C. Yau, P.W. Laird, L. Ding, W. Zhang, G. B. Mills, R. Kucherlapati, E.R. Mardis, D.A. Levine, Integrated genomic characterization of endometrial carcinoma, Nature 497 (2013) 67–73.
[44] A. León-Castillo, H. Britton, M.K. McConechy, J.N. McAlpine, R. Nout, S. Kommoss, S.Y. Brucker, J.W. Carlson, E. Epstein, T.T. Rau, T. Bosse, D.N. Church, C. B. Gilks, Interpretation of somatic POLE mutations in endometrial carcinoma, J. Pathol. 250 (2020) 323–335.
[45] R.X. Huang, P.K. Zhou, DNA damage response signaling pathways and targets for radiotherapy sensitization in cancer, Signal Transduct. Targeted Ther. 5 (2020) 60.
[46] J.A. Nickoloff, N. Sharma, C.P. Allen, L. Taylor, S.J. Allen, A.S. Jaiswal, R. Hromas, Roles of homologous recombination in response to ionizing radiation-induced DNA damage, Int. J. Radiat. Biol. 99 (2023) 903–914.
[47] J. Monge-Cadet, E. Moyal, S. Supiot, V. Guimas, DNA repair inhibitors and radiotherapy, Cancer Radiother. : journal de la Societe francaise de radiotherapie oncologique 26 (2022) 947–954.
[48] M. Hom-Tedla, R.N. Eskander, Immunotherapy treatment landscape for patients with endometrial cancer: current evidence and future opportunities, Clin. Adv. Hematol. Oncol. : H&O 21 (2023) 27–34.
[49] T.C. Longoria, R.N. Eskander, Immunotherapy in endometrial cancer - an evolving therapeutic paradigm, Gynecologic oncology research and practice 2 (2015) 11.
[50] B. Pirš, E. Škof, V. Smrkolj, Š. Smrkolj, Overview of immune checkpoint inhibitors in gynecological cancer treatment, Cancers 14 (2022).
[51] H. Ghebeh, S. Mohammed, A. Al-Omair, A. Qattan, C. Lehe, G. Al-Qudaihi, N. Elkum, M. Alshabanah, S. Bin Amer, A. Tulbah, D. Ajarim, T. Al-Tweigeri, S. Dermime, The B7-H1 (PD-L1) T lymphocyte-inhibitory molecule is expressed in breast cancer patients with infiltrating ductal carcinoma: correlation with important high-risk prognostic factors, Neoplasia 8 (2006) 190–198.
[52] B.S. Jang, I.A. Kim, A radiosensitivity gene signature and PD-L1 predict the clinical outcomes of patients with lower grade glioma in TCGA, Radiother. Oncol. : journal of the European Society for Therapeutic Radiology and Oncology 128 (2018) 245–253.